

PACS 73.22.-f, 78.67.Bf

Optical spectra of small CdS nanocrystals

V.I. Boichuk, R.Ya. Leshko, V.B. Holskyi, D.S. Karpyn

Ivan Franko Drohobych State Pedagogical University,

Department of theoretical and applied physics, and computer simulation

3, Stryiska str., 82100 Drohobych, Lviv Region, Ukraine

Abstract. Determined in this work is the energy of surface states related with polarization charges at the interfaces. This energy was compared with that of electron internal states. Dipole momentum matrix elements of the interlevel transition were also determined. The value of interlevel absorption coefficient versus the electromagnetic wave frequency was calculated.

Keywords: polarization trap, quantum dot, surface states.

Manuscript received 21.07.16; revised version received 15.09.16; accepted for publication 16.11.16; published online 05.12.16.

1. Introduction

Already several decades, physics of quasi-zero-dimension semiconductor clusters (nanocrystals, quantum dots) causes evident interest of researchers [1, 2]. Low dimensions of the system evoke a number of interesting changes of physical characteristics inherent to crystals. Among their numerous properties, one can obtain discrete structure of the electron, hole and exciton energy spectrum. The main condition must be true – nanocrystal size is smaller than radius of Wannier–Mott exciton in bulk crystals [2-5]. During investigation, quasi-particle energy levels, spectroscopy methods play an important role. Currently, detailed researches confirm the strength quantum restriction particle regime existence in nanocrystals.

In this study, a significant place is paid to heterostructures with CdS quantum dots (QDs). These QDs can substitute organic substance in the biologic sensors and be used in other optical electronic devices. Therefore, in recent years many researchers paid attention to elaborate new technology to produce high-quality and stable CdS QDs in solid state and polymer matrixes.

Many works [4-14] are devoted to investigations of CdS nanocrystal photoluminescence properties. It was shown that CdS QDs in polymer matrix contain their own defects of two types. It indicated by red and green region luminescence. It was determined that defects $Cd_iV_{Cd}-V_S$ are reason for the existence mentioned optic bands in bulk CdS crystals. The analyses of experimental data show that the physical nature of the matrix does not influence on the type of radiation centers in QD [15, 16]. But it was shown that the matrix plays a significant role in the process of luminescence stimulating. Specifically, the gelatin presence strongly increases the intensity of red luminescence.

The heterosystem interfaces play an important role in optical properties of QD system. Reducing the size of QDs is accompanied by the increasing role of surfaces in absorption and luminescence spectra. In many physical situations, the red part of radiation spectrum is not caused by the interband transitions, but caused by electrons transition with participation of surface traps [14].

In majority of works devoted QD luminescence phenomenon various reasons for the surface states appearance were considered. Among them, it was discussed availability of broken bonds as well as absorbed

atoms in the systems [11-12]. Another reason for appearance of surface states is interaction of charged particles and coupling surface charges at the heterostructure interfaces [17-18]. The physical conditions for manifestation of these states are studied less.

In this paper, we study CdS/SiO₂ heterostructure with spherical QDs. The energy of interface states has been calculated. Models of abrupt and fluent coordinate changes of a dielectric permittivity near surface of QD were considered. The effect of interface states on the interlevel absorption coefficient has been studied.

2. Potential energy of the charged particle in QD/matrix heterosystem

Let us consider heterosystem consisting of a dielectric or semiconductor matrix that contains spherical QDs. Every charged particle is characterized by its own effective mass in each medium (m_1^* , m_2^*). The media are described by their own dielectric permittivity (ε_1 , ε_2).

Modern technology enables to obtain sufficient quality of semiconductor and dielectric nanoheterostructures. In reality, it is difficult to create a heterogeneous system with sharp changes in all physical parameters at the interface, where particle's coordinate $r = a$ (a is the QD radius). There is always an intermediate layer, in which a particular physical parameter (particle's effective mass, dielectric constant) varies in its value from one crystal to another.

2.1. Heterosystem with the sharply varying dielectric permittivity at the interface

We simplify the model by assuming that in the point $r = a$ the dielectric permittivity is abruptly varied. That is

$$\varepsilon(r) = \varepsilon_1 \theta(a-r) + \varepsilon_2 \theta(r-a), \quad r \geq a, \quad (1)$$

where $\theta(x)$ is the Heaviside function. The potential in the system QD/matrix can be found, if one solves the Poisson and Laplace equations as in [15]:

$$\Phi(\vec{r}, \vec{r}_0) = \begin{cases} \Phi_1(\vec{r}, \vec{r}_0), & r < a, \\ \Phi_2(\vec{r}, \vec{r}_0), & r > a, \end{cases} \quad (2)$$

where \vec{r} , \vec{r}_0 are the radius-vectors of an arbitrary point in the space and the particle, respectively. As known, bound charges can arise at the interfaces of the nonhomogeneous environment. The can obtain surface density of these charges by using the polarization boundary condition:

$$\sigma = P_{1n} - P_{2n} = \frac{1}{4\pi} \left(\frac{\partial \Phi_1(\vec{r}, \vec{r}_0)}{\partial r} - \frac{\partial \Phi_2(\vec{r}, \vec{r}_0)}{\partial r} \right) \Bigg|_{r=a}. \quad (3)$$

The potential energy of $q = 1$ charge interacting with surface bound charges, arising from the existence of the same charge, is determined by the formula [15]:

$$V_p(r) = \begin{cases} \frac{1}{2a\varepsilon_1} \frac{\varepsilon_1 - \varepsilon_2}{\varepsilon_1 + \varepsilon_2} \left[\frac{a^2}{a^2 - r^2} + \frac{\varepsilon_1}{\varepsilon_2} \times \right. \\ \left. \times F \left(1, \frac{\varepsilon_2}{\varepsilon_1 + \varepsilon_2}; \frac{\varepsilon_2}{\varepsilon_1 + \varepsilon_2} + 1; \left(\frac{r}{a} \right)^2 \right) \right], & r < a, \\ \frac{1}{2a\varepsilon_2} \frac{\varepsilon_1 - \varepsilon_2}{\varepsilon_1 + \varepsilon_2} \left[\frac{a^2}{a^2 - r^2} + \left(\frac{a}{r} \right)^2 \times \right. \\ \left. \times F \left(1, \frac{\varepsilon_2}{\varepsilon_1 + \varepsilon_2}; \frac{\varepsilon_2}{\varepsilon_1 + \varepsilon_2} + 1; \left(\frac{a}{r} \right)^2 \right) \right], & r > a, \end{cases} \quad (4)$$

where F is the hypergeometric function. Analysis of (4) shows that, for the small particle distance to the interface, the first term is valid in both situations: if $r < a$ or $r > a$. In addition, the function $V_p(r)$ includes a non-physical discontinuity in the point $r = a$. If the inequality $\varepsilon_1 > \varepsilon_2$ is true, then the potential $V_p(r)$ can be represented by the function like to that in Fig. 1. Otherwise, the coordinate dependence of the potential changes. It will be characterized by the opposite sign.

2.2. Heterosystem with the smoothly varying dielectric permittivity at the interface

Let at the interface exists an intermediate layer where dielectric permittivity changes from its value in QD to the corresponding matrix value. In this case, one may repeat calculation of [16] and obtain the potential energy of interaction of the charged particle and polarization charges in the following look:

$$V_p(r) = \frac{\gamma}{4\varepsilon(r)} \int_0^\infty dr_0 \frac{\text{th} \left(\frac{r_0 - a}{L} \right) + \frac{r_0}{L} \text{sech}^2 \left(\frac{r_0 - a}{L} \right)}{r_0^2 - r^2}, \quad (5)$$

$$\varepsilon(r) = \frac{\varepsilon_1 + \varepsilon_2}{2} \left[1 - \gamma \text{th} \left(\frac{r - a}{L} \right) \right], \quad (6)$$

$$\gamma = \frac{\varepsilon_1 - \varepsilon_2}{\varepsilon_1 + \varepsilon_2}. \quad (7)$$

Based on the formula (5), the analysis shows that the width of the intermediate layer is close to the lattice parameter a_0 , when $L \leq 1/4a_0$. In Figs. 1 and 2, the potential $V_p(r)$ based on the expressions (4) and (5) is shown as a function of the coordinate r .

3. Schrödinger equation of the charged particle (electron) in the heterosystem

We consider the electron of CdS spherical QD in the matrix SiO₂. We write the Hamiltonian of the system using Hartree units ($m_0 = 1$, $\hbar = 1$, $e = 1$):

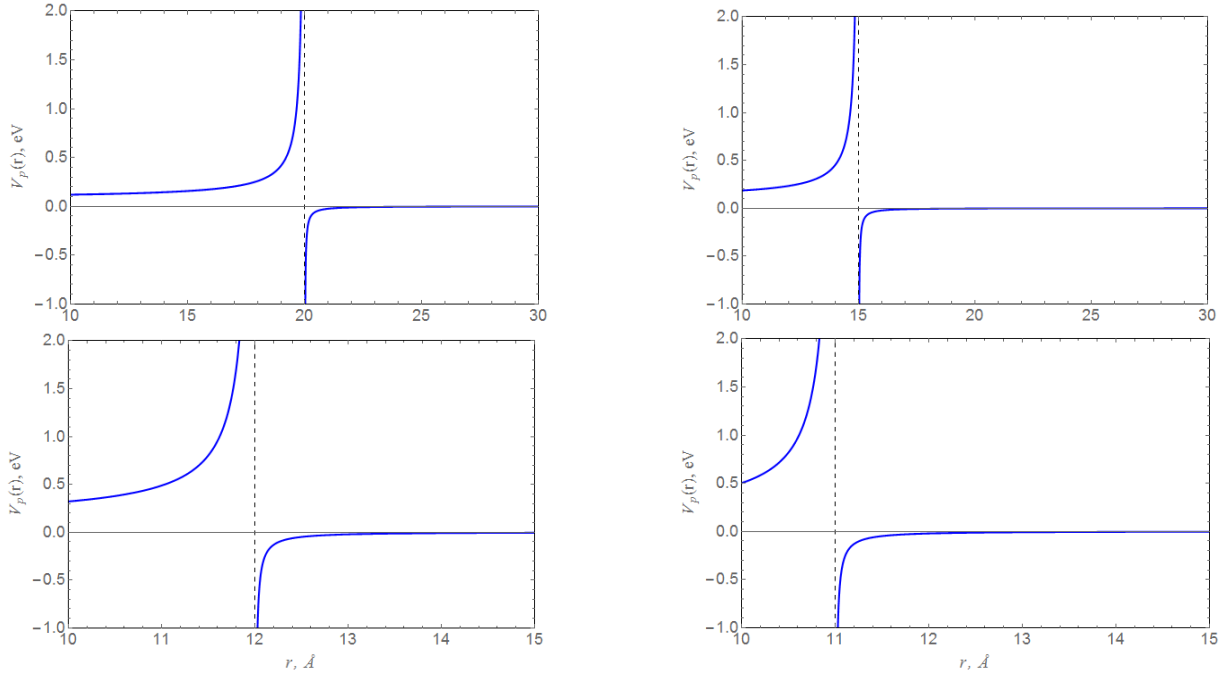


Fig. 1. Potential (4) for different values of the QD radius.

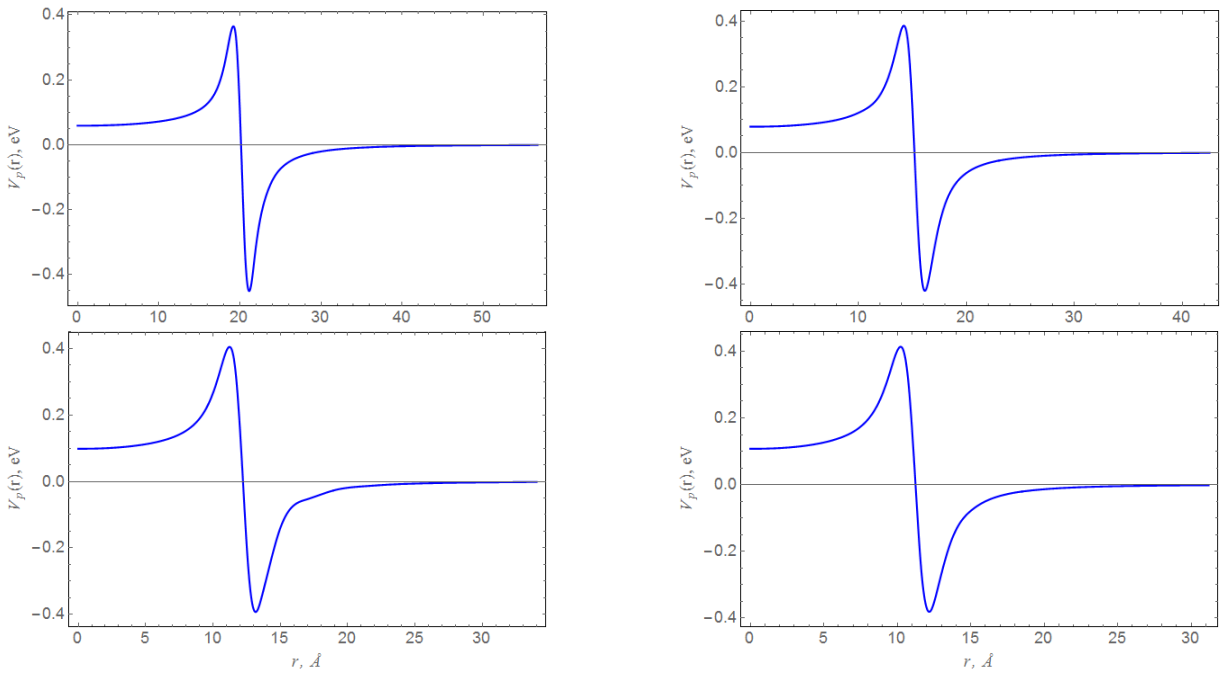


Fig. 2. Potential (5) for different values of the QD radius.

$$\hat{\mathbf{H}} = -\frac{1}{2} \nabla \frac{1}{m(r)} \nabla + U(r) + V_p(r), \quad (8)$$

where the confinement potential is

$$U(r) = \begin{cases} 0, & r \leq a, \\ U_0, & r > a, \end{cases} \quad (9)$$

and the potential energy $V_p(r)$ is expressed by (4) or (5). Taking into account the view of total potential energy

$(U(r) + V_p(r))$ as the function of the coordinate r , it can be assumed that the charge can be localized both in the middle and outside QD.

At first, we solve the Schrödinger equation (SE) with the Hamiltonian (8) and potential (4) (a self-action potential). Since the self-action potential contains discontinuity in the point $r = a$, we solve SE alone in the middle and outside QD.

Let the electron is in QD. Under the guide of the self-action potential, the charge cannot go beyond QDs.

So, we replace the finite potential (9) by an infinite one. The self-action potential in SE is a small perturbation. In zeroth approximation, this equation has an analytical solution:

$$\begin{aligned} \Psi_{e;n,l,m}^{in}(\vec{r}_e) &= R_{e;n,l}(r_e)Y_{l,m}(\Omega_e) = \\ &= A_{n,l} j_l(k_{n,l} r_e / a) Y_{l,m}(\Omega_e), \end{aligned} \quad (10)$$

$$E_{n,l} = \frac{k_{n,l}^2}{2m_1^* a^2}. \quad (11)$$

k_{nl} is n -th zero of spherical Bessel function $j_l(x)$. The self-action potential can be considered as a first approximation of the perturbation theory. Therefore,

$$E_{n,l}^{in} = \frac{k_{n,l}^2}{2m_1^* a^2} + \langle n,l | V_p | n,l \rangle. \quad (12)$$

The electron can be also outside QD in the so-called polarization trap. We use the variational Ritz method to determine the ground state particle energy. The variation trial function

$$\Psi_{e;n,l,m}^{out}(\vec{r}_e) = C(r_e - a)e^{-\alpha(r_e - a)^2}, \quad r_e \geq a \quad (13)$$

with the variational parameter α allows calculating the particle energy E_{10}^{out} . The plots of particle energy dependences versus the QD radius are shown in Fig. 3. These plots show that for the selected model the electron energy of the state (13) is higher than that of outward bound state (10). Moreover, we have obtained different QD radius dependences of the electron energy in the considered states. So, if the energy $E_{1,0}^{in} \sim a^{-2}$, the energy $E_{1,0}^{out}$ is characterized by a weak radius change. Calculations have shown that reducing the QD radius involves a reduction of $\min \alpha$. It means the increase of the electron average distance to the QD surface. So, at small radius ($a < 10$ E) outward bound electron state disappears. It is possible under certain conditions quantum transition of electron from the external to internal states, if $a > 10$ E.

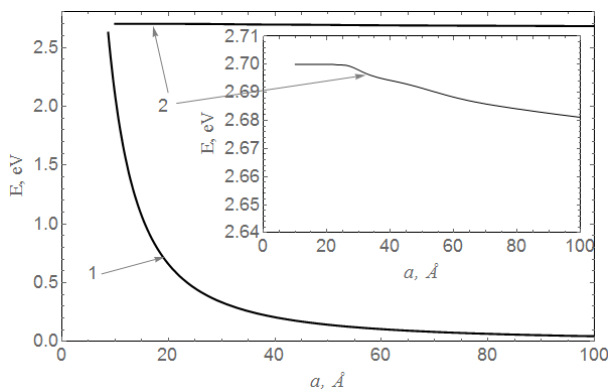


Fig. 3. Electron energy of the ground state E^{in} (1), E^{out} (2).

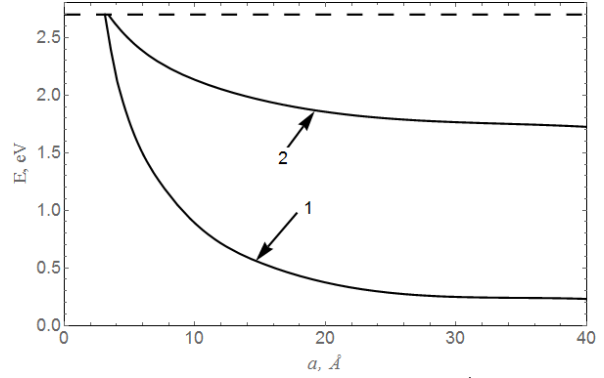


Fig. 4. Electron energy of the ground state E^{in} (1), E^{out} (2) obtained using the potentials (5) and (9). Horizontal dashed line corresponds to U_0 (9).

It is opportunity to do analysis of SE for the model with potentials (9) and (5). We take into account that the potential (5) is the small perturbation in this problem. In zeroth approximation, the solution of SE can be written as in [16]

$$\begin{aligned} \Psi_{e;n,l,m}(\vec{r}_e) &= R_{e;n,l}(r_e)Y_{l,m}(\Omega_e) = \\ &= \begin{cases} A_{n,l} j_l(k_{n,l} r_e / a), & r_e \leq a \\ B_{n,l} k_l(x_{n,l} r_e / a), & r_e > a \end{cases} \times Y_{l,m}(\Omega_e), \end{aligned} \quad (14)$$

where

$$k_{n,l} = a\sqrt{2m_{e1}^* E_{e;n,l}}, \quad x_{n,l} = a\sqrt{2m_{e2}^* (U_0 - E_{e;n,l})},$$

and $j_l(x)$, $k_l(x)$ are the spherical Bessel functions. We found the electron energy from the boundary conditions (without discontinuity in the wave functions and probability density flux on the QD surface). In this approach, electron even in the ground state with a certain probability can penetrate from QD into the matrix, because the wave function “tail” is not equal zero in the matrix space due to finite particle confinement. As in the previous part of the paper, the electron energy has found using the perturbation theory:

$$E_{n,l} = E_{e;n,l} + \langle n,l | V_p | n,l \rangle. \quad (15)$$

If electron is outside QD (in the polarization trap), the variational problem can be also solved. In this case, the trial function of s -type was chosen in the form

$$\Psi_{100}^{out}(\vec{r}_e) = D \exp \left[-\beta \left(\frac{r}{a} - 1 \right)^2 \right]. \quad (16)$$

Choosing the wave function in the form (16) provides decreasing the wave function versus the distance from a boundary of QD in both directions (a bound interface state of electron).

In Fig. 4, one can see the dependence of the electron energy on the radius of QD for the inside (14)

and outside (16) problems. As seen in Fig. 4, the energy of bound electron (curve 2) is higher than that of the electron ground state. This result is similar to that of the previous model. But there is a quantitative difference. As Fig. 4 shows, for $a = 20$ E the electron energy of the ground state ~ 0.4 eV and of the bound interface state ~ 2 eV. The similar energy values for the first model (Fig. 3) are 0.5 eV and 2.7 eV. We have a considerable energy difference.

For future investigation, we will calculate the energies and wave functions p -types of the electron in polarization trap. This trial function can be chosen like to (16):

$$\psi_{110}^{out}(\vec{r}_e) = G \cos(\theta_e) \exp\left[-\gamma \left(\frac{r_e}{a} - 1\right)^2\right]. \quad (17)$$

Minimizing the corresponding functional, one obtains the electron energy and wave function of the bound interface p -state. The same calculations can be also carried out for inside problem by using Exps (14) and (15). The electron energy of all these states are monotonous functions of the DQ radius (Fig. 5). We obtain the degeneracy of the electron spectrum in QD for the fixed radii: $a = 20, 32, 43$ E and so on.

4. Interlevel transitions and light absorption of the heterosystem

Let the heterosystem is irradiated by the linearly polarized light along z direction. Then, in the dipole approximation the interlevel transitions are possible between states where $\Delta l = \pm 1$ and $\Delta m = 0$. For the QD radius 18 E (exciton radius CdS is equal 16.9 E), we calculate the energy levels and show all the possible transitions in Fig. 6. In this case, there possible are 8 transitions that are caused of absorption of light. Therefore, the density matrix and iterative procedure were applied to derive the absorption coefficient [19-21]. In this approach, the linear absorption coefficient can be expressed as

$$\alpha_{m,n}(\omega) = \omega \sqrt{\frac{\mu_0}{\varepsilon_0 \varepsilon}} \frac{N |d_{mn}|^2 \hbar \Gamma}{(E_n - E_m - \hbar \omega)^2 + (\hbar \Gamma)^2}, \quad (18)$$

where ε_0 is the electric constant of vacuum, μ_0 – magnetic constant of vacuum, c – light speed, $\square \Gamma$ is the scattering rate caused by the electron-phonon interaction and some other factors of scattering. If $T \approx 4$ K and $\square \Gamma$ limits to zero, one can obtain:

$$\begin{aligned} \alpha_{m,n}(\omega) &= \lim_{\hbar \Gamma \rightarrow 0} \left(\omega \sqrt{\frac{\mu_0}{\varepsilon_0 \varepsilon}} \frac{N |d_{mn}|^2 \hbar \Gamma}{(E_n - E_m - \hbar \omega)^2 + (\hbar \Gamma)^2} \right) = \\ &= \omega \pi \sqrt{\frac{\mu_0}{\varepsilon_0 \varepsilon}} N |d_{mn}|^2 \delta(E_n - E_m - \hbar \omega). \end{aligned} \quad (19)$$

$N \approx 3 \square 10^{16} \text{ cm}^{-3}$ is carrier concentration.

In practice, QDs sets are obtained as located in a crystal or polymer matrix. Whatever method of cultivation is used, the set of QDs is always characterized by the size dispersion. Let the QD size distribution is approximated by the Gauss function:

$$g(s, \bar{a}, a) = \frac{1}{s\sqrt{2\pi}} \exp\left(-\frac{(a - \bar{a})^2}{2s^2}\right), \quad (20)$$

where a is the QD radius (variable), s – halfwidth of the distribution (20), which is expressed by the average radius \bar{a} and value σ that is considered as the variance in the QD sizes expressed in percent: $s = \bar{a}\sigma/100$. By regarding the QD dispersion (20), the absorption coefficient can be obtained for the QDs set by using the following expression

$$\begin{aligned} \alpha_{m,n,system}(\omega) &= \omega \pi \sqrt{\frac{\mu_0}{\varepsilon_0 \varepsilon}} \times \\ &\times N \int g(s, \bar{a}, a) |d_{mn}|^2 \delta(E_n(a) - E_m(a) - \hbar \omega) da. \end{aligned} \quad (21)$$

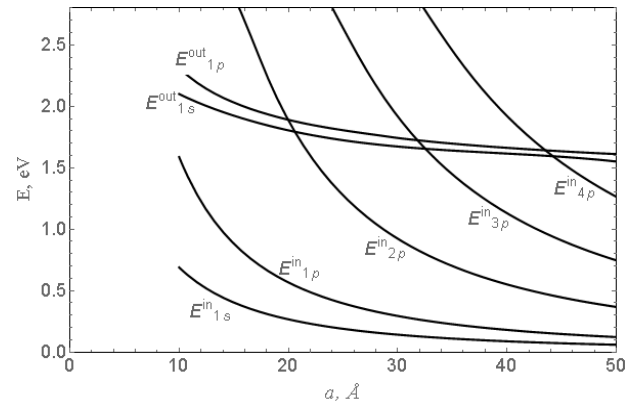


Fig. 5. Electron energies of the ground and excited p -states in the heterosystem.

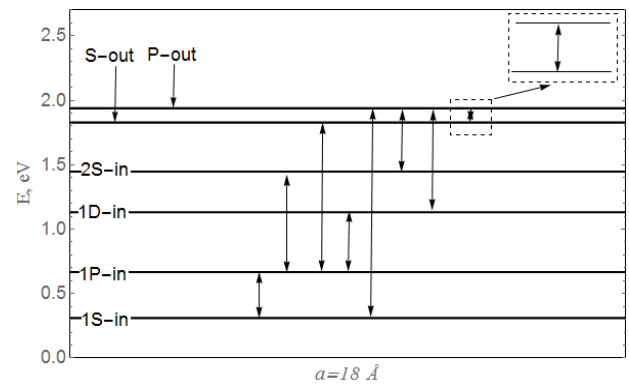


Fig. 6. Quantum transitions in the heterosystem. Average radius of QD is 18 E.

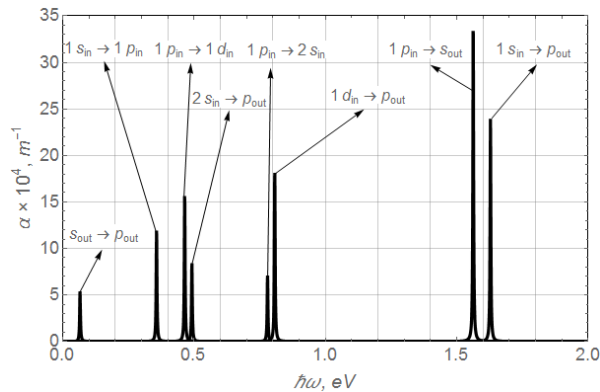


Fig. 7. Light absorption coefficient of the heterosystem. Average radius of QD is 18 E, $\sigma = 3\%$.

With account of delta-function properties, one can obtain:

$$\alpha_{m,n;system}(\omega) = \omega\pi \sqrt{\frac{\mu_0}{\epsilon_0\epsilon}} N \int g(s, \bar{a}, a) |d_{mn}|^2 \times \\ \times \sum_i \frac{\delta(a - a_{0i})}{\left| \frac{d}{da} (E_n(a) - E_m(a) - \hbar\omega) \right|_{a=a_{0i}}} da,$$

where a_{0i} are simple zeros of the function $F(a) = (E_n(a) - E_m(a) - \hbar\omega)$. Therefore,

$$\alpha_{m,n;system}(\omega) = \\ = \omega\pi \sqrt{\frac{\mu_0}{\epsilon_0\epsilon}} N \sum_i \frac{g(s, \bar{a}, a_{0i}) |d_{mn}(a_{0i})|^2}{\left| \frac{d}{da} (E_n(a) - E_m(a) - \hbar\omega) \right|_{a=a_{0i}}}. \quad (22)$$

The dependence of the absorption coefficient on the energy of light quanta for the QD average radius and dispersion $\sigma = 3\%$ was plotted using the expression (22). Fig. 7 shows coefficients of light absorption for all possible transition cases. The plots show narrow absorption bands. If $\sigma = 10\%$, the absorption bands become wide, that is why $1p_{in} \rightarrow 1d_{in}$ and $2s_{in} \rightarrow p_{out}$; $1p_{in} \rightarrow 2s_{in}$ and $1d_{in} \rightarrow p_{out}$; $1p_{in} \rightarrow s_{out}$ and $1s_{in} \rightarrow p_{out}$ begin merge. In both cases, $\sigma = 3\%$ and 10% one can observe the absorption band caused by the transition from the external surface states into the internal ones. But in the first case ($\sigma = 3\%$) there are two bands and in the second – one merged band. In all the cases, one can differ the absorption bands caused by the interface states and QD states. Also, we can signify that this transition should effect on the photoluminescence spectra, which will be studied in our next works.

References

1. A.I. Yekimov, A.A. Onushchenko, Quantum-sized effect in three-dimensional microcrystals of
2. A.I. Savchuk, V.V. Makovii, Influence of doping the CdS colloid nanoparticles with Mn impurity on their photoluminescence spectra // *Naukovyi visnyk Chernivetskoho natsionalnoho universytetu: Fizyka, elektronika*, **2**(1), p. 66-68 (2012), in Ukrainian.
3. D.V. Korbutiak, O.V. Kovalenko, S.I. Budzuliak et al., Light-emitting properties of quantum dots made of semiconductor compounds A_2B_6 // *Ukr. J. Phys.* **7**(1), p. 48-95 (2012).
4. M. Romcevic, N. Romcevic, R. Kostic et al., Photoluminescence of highly doped $Cd_{1-x}Mn_xS$

- semiconductors // *Pis'ma v ZhETF*, **34**(6) p. 363-366 (1981), in Russian.
2. A.I. Efros, A.L. Efros, Interband light absorption in a semiconductor sphere // *Fizika i tekhnika poluprovodnikov*, **16**(7), p. 1209-1214 (1982), in Russian.
3. Y. Kayanuma, Quantum-size-effects of interaction electrons and holes in semiconductor microcrystals with spherical shape // *Phys. Rev. B*, **38**(14), p. 9797-9805 (1989).
4. P. Nandakumar, C. Vijayan, Y.V.G.S. Murti, Optical absorption and photoluminescence studies an CdS quantum dots in Nafion // *J. Appl. Phys.* **91**(3), p. 1509-1514 (2002).
5. D.O. Demchenko and Lin-Wang Wang, Optical transitions and nature of Stokes shift in spherical CdS quantum dots // *arXiv:cond-mat/0603563v1* [cond-mat.mtrl-sci] (2006).
6. V.M. Skobeleva, V.A. Smyntyna, O.I. Sviridova et al., Optical properties of cadmium sulfide nanocrystals prepared using the sol-gel method in gelatin // *Zhurnal prikladnoi spektroskopii*, **75**(4), p. 556-562 (2008), in Russian.
7. V. Smyntyna, B. Semenenko, V. Skobeleva, N. Malushin, Influence of CdS nanocrystals surface on their luminescent properties // *Elektronika ta informatsiini tekhnologii*, №2, p. 45-50 (2012), in Ukrainian.
8. V.A. Smyntyna, V.M. Skobeleva, N.V. Malushin, Luminescent properties of cadmium sulfide nanocrystals doped with lithium and aluminum atoms // *Sensorna elektronika ta mikrosistemni tekhnologii*, **2**(8), p. 55 (2011), in Ukrainian.
9. V. Smyntyna, V. Skobeleva, N. Malushin, The nature of emission centers in CdS nanocrystals // *Radiation Measurements*, **42**, p. 693-696 (2007).
10. V.I. Fediv, G.Yu. Rudko, A.I. Savchuk, E.G. Gule, A.G. Voloshchuk, Synthesis route and optical characterization of CdS:Mn/polyvinyl alcohol nanocomposite // *Semiconductor Physics, Quantum Electronics and Optoelectronics*, **15**(2), p. 117-123 (2012).
11. D.V. Korbutiak, S.V. Tokarev, S.I. Budzuliak et al., Optical and structure-defect characteristics of CdS:Cu i CdS:Zn nanocrystals synthesized in polymer matrixes // *Fizyka i khimiiia tverdoho tila*, **14**(1), c. 222-227 (2013), in Ukrainian.
12. A.I. Savchuk, V.V. Makovii, Influence of doping the CdS colloid nanoparticles with Mn impurity on their photoluminescence spectra // *Naukovyi visnyk Chernivetskoho natsionalnoho universytetu: Fizyka, elektronika*, **2**(1), p. 66-68 (2012), in Ukrainian.
13. D.V. Korbutiak, O.V. Kovalenko, S.I. Budzuliak et al., Light-emitting properties of quantum dots made of semiconductor compounds A_2B_6 // *Ukr. J. Phys.* **7**(1), p. 48-95 (2012).
14. M. Romcevic, N. Romcevic, R. Kostic et al., Photoluminescence of highly doped $Cd_{1-x}Mn_xS$

- nanocrystals // *J. Alloys and Compounds*, **497**, p. 46-54 (2010).
15. V.I. Boichuk, P.Yu. Kubai, I.V. Bilynskyi, Influence of the image potential on the energy spectrum of electron in complex spherical microcrystal CdS/beta-HgS/H₂O // *Zhurnal fizychnykh doslidzhen'*, **3**(2), p. 187-191 (1999), in Ukrainian.
 16. V.I. Boichuk, R.Yu. Kubai, Effect of an intermediate layer with space-dependent permittivity on the ground state energy of an electron in a spherical complex nanoheterosystem // *Physics of the Solid State*, **43**(2), p. 235-241 (2001).
 17. V.I. Boichuk, I.V. Bilynskyi, R.Ya. Leshko et al., The effect of the polarization charges on the optical properties of a spherical quantum dot with an off-central hydrogenic impurity // *Phys. E: Low-dim. Systems and Nanostruct.* **45**(2), p. 476-482 (2011).
 18. V.I. Boichuk, I.V. Bilynskyi, R.Ya. Leshko et al., Optical properties of a spherical quantum dot with two ions of hydrogenic impurity // *Phys. E: Low-dim. Systems and Nanostruct.* **54**, p. 281-287 (2013).
 19. M.R.K. Vahdani, and G. Rezaei, Linear and nonlinear optical properties of a hydrogenic donor in lens-shaped quantum dots // *Phys. Lett. A*, **373**(34), p. 3079-3084 (2009).
 20. G. Rezaei, M.R.K. Vahdani, and B. Vaseghi, Nonlinear optical properties of a hydrogenic impurity in an ellipsoidal finite potential quantum dot // *Current Appl. Phys.* **11**(2), p. 176-181 (2011).
 21. C.L. Tang, *Fundamentals of Quantum Mechanics for Solid State Electronics and Optics*. Cambridge University Press, Cambridge, 2005.